Journal of Experimental Agriculture International

43(4): 120-144, 2021; Article no.JEAI.69364
ISSN: 2457-0591
(Past name: American Journal of Experimental Agriculture, Past ISSN: 2231-0606)

Use of PhenoCam Measurements and Image Analysis to Inform the ALMANAC Process-based Simulation Model

Jacqueline Jacot[1*], James R. Kiniry[2], Amber S. Williams[2], Addison Coronel[3], Jianzhong Su[3], Gretchen R. Miller[4], Binayak Mohanty[5], Amartya Saha[6], Nuria Gomez-Casanovas[7], Jane M. F. Johnson[8] and Dawn M. Browning[9]

[1]Oak Ridge Institute for Science and Education, 808 East Blackland Rd., Temple, TX 76502, USA.
[2]USDA, Agricultural Research Service, Grassland Soil and Water Research Laboratory, 808 East Blackland Rd., Temple, TX 76502, USA.
[3]Department of Mathematics, University of Texas in Arlington, 701 S. Nedderman Drive, Arlington, TX 76019, USA.
[4]Zachry Department of Civil & Environmental Engineering, Texas A&M University 3136 TAMU, College Station, TX 77843-3136, USA.
[5]Biological and Agricultural Engineering Department, Texas A&M University 2117 TAMU, College Station, TX 77843-2117, USA.
[6]Archbold Biological Station, Buck Island Ranch, 300 Buck Island Ranch Road, Lake Placid, FL 33852, USA.
[7]University of Illinois Urbana Champaign, USA.
[8]Agricultural Research Service, North Central Soil Conservation Research Laboratory, USDA, 803 Iowa Ave, Morris, MN 56267, USA.
[9]Agricultural Research Service, Jornada Experimental Range, USDA, Las Cruces, NM 88003, USA.

Authors' contributions

This work was carried out in collaboration among all authors. Author JJ designed the study, wrote the protocol, wrote the first draft of the manuscript and provided revisions. Author JRK designed the study, wrote the protocol, wrote the first draft of the manuscript, and provided revisions. Author ASW designed the study, wrote the protocol, wrote the first draft of the manuscript, and provided revisions. Author AC designed the study, wrote the protocol and provided revisions. Author JS designed the study and provided revisions. Author GRM curated data and provided revisions. Author BM curated data and provided revisions. Author AS curated data and provided revisions. Author NG-C curated data and provided revisions. Author JMFJ curated data and provided revisions. Author DMB designed the study, curated data, and provided revisions. All authors read and approved the final manuscript.

Article Information

DOI: 10.9734/JEAI/2021/v43i430684
Editor(s):
(1) Prof. Mohamed Fadel, National Research Center, Egypt.
Reviewers:
(1) Isaeva Oksana Leonidovna, Yugra State University, Russia.
(2) Formeluh Abraham Toh, University of Buea, Cameroon.
Complete Peer review History: http://www.sdiarticle4.com/review-history/69364

**Corresponding author: E-mail: Jacqueline.Jacot@usda.gov;*

Original Research Article

Received 14 April 2021
Accepted 18 June 2021
Published 05 July 2021

ABSTRACT

Near-surface remote sensing has been used to document seasonal growth patterns (i.e. phenology) for plant communities in diverse habitats. Phenology from this source may only apply to the area within the images. Meanwhile ecosystem models can accommodate variable weather and landscape differences to plant growth, but accuracy is improved by adding ground-truthed inputs. The objective of this study was to use PhenoCam data, image analysis, and Beer's law with established extinction coefficients to compare leaf area index (LAI) development in the ALMANAC model for diverse plant types and environments. Results indicate that PhenoCam time series imagery can be used to improve leaf area development in ALMANAC by adjusting parameter values to better match LAI derived values in new diverse environments. Soybeans, mesquite, and maize produced the most successful match between the model simulations and PhenoCam data out of the eight species simulated. This study represents, to our knowledge, the first independent evaluation of the ALMANAC process-based plant growth model with imagery in agroecosystems available from the PhenoCam network. The results show how PhenoCam data can make a valuable contribution to validate process-based models, making these models much more realistic and allows for expansion of PhenoCam influence.

Keywords: PhenoCam Network; ALMANAC model; ImageJ; phenology; green chromatic coordinate; Leaf Area Index (LAI)

1. INTRODUCTION

Analysis of time series photography allows us to track changes in ecosystems over time enabling us to extrapolate data and measure occurring changes. Plant phenology, specifically, the development of leaf area cover over time, is a primary determinant of plant productivity for all plants in all environments. The seasonal growth curve, beginning with spring greenup, through maximum leaf area cover (often near anthesis), and finally, at the end of the growing season (senescence) determines the amount of plant biomass produced, the amount of water transpired, and is the driver for many environmental aspects. Two parallel approaches to quantifying plant phenology have been direct measurement by daily color pictures and the simulation by process models relying on plant parameters, soils data, and weather data. Our goal is to quantify how much green is in photographs of specific plants and to calculate leaf area index (LAI) and relate it to values from model simulations. Ideally, both the LAI calculation and the model should show similar phenological seasonality and have similar LAI values for the plants.

The PhenoCam Network is a series of over 600 high-resolution digital cameras installed at locations in North America which take photos every thirty minutes and transmit them to an open access repository (https://phenocam.sr.unh.edu/webcam/).

Although the project began as a way to monitor forests in the northeastern United States, they now function as "a continental-scale phenological observatory, spanning as wide a range of biogeoclimatic zones and vegetation types as possible" [1]. This near-surface remote sensing provides several advantages to conventional remote sensing, including being nearly continuous in time and being free of obstructions like clouds or atmospheric effects. Thus, it has been studied and applied to many research concepts like green up [2–4] and canopy cover [5,6] in habitats from deciduous forests to cold deserts to rice paddies and arid ecosystems. Data from PhenoCams, including non-photographic data such as Green Chromatic Coordinate (GCC) and Regions of Interest (ROIs), are used to link field and satellite observations of landscape phenology. These data have been used to constrain model parameters in North American grasslands but it could theoretically be used to bolster modelling techniques in a multitude of ecosystems [7,8].

The ALMANAC model has already been applied to a wide variety of crops, grasses, and woody vegetation. ALMANAC, or Agricultural Land

Management Alternative with Numerical Assessment Criteria, can simulate plant growth, competition, light interception by leaves, biomass accumulation, partitioning of biomass into grain, water use, nutrient uptake, and growth constraints such as water, temperature, and nutrient stresses [9]. Light interception by the leaf canopy is simulated with Beer's law [10] and the LAI. The greater the value of the extinction coefficient k, the more light will be intercepted at a given LAI. The fraction (Fraction) of incoming solar radiation intercepted by the leaf canopy is

$$\text{Fraction} = 1.0 - \exp(k * \text{LAI}). \quad (1)$$

The extinction coefficient (k) is the only fitted variable.

ALMANAC requires inputs of soil, weather, tillage, and plant parameters, utilizing these real-world data improves its accuracy [9]. It is common to use default ALMANAC plant parameters for new simulations that have been derived from years of field measurements, but adjustments for degree days for the growing season (PHU) are typically applied when moving to new sites. The direct method of measuring LAI and other parameters can take considerable time and resources to establish by visiting sites throughout the growing season across several years. Plant growth parameters based on these initial collections are calibrated and validated and added to the model's database. Plant parameters transferred to different growing conditions sometimes requiring a few additional modeling adjustments such as the planting density or speed of the growth curve for LAI. Being able to model plant growth is extremely beneficial for addressing questions in management, site selection, climate change, phenology, and yield. Collecting data can be costly in terms of time and travel so PhenoCams can help optimize the model for new areas with less costs. This study shows how LAI derived from PhenoCams can increase the accuracy of the model by providing accurate timing of plant phenology from new distant sites. Thus, ALMANAC will have field data to compare without intense trials, as baseline plant parameters have already been established and only need minor adjustments to new locations. Likewise, PhenoCams are only accurate for the plants seen within the photo, but with the ALMANAC model's help, seasonal changes can be extrapolated for a much larger landscape.

Linking these two systems, the PhenoCam Network and the ALMANAC model, advance quantification of plant phenology. Just as PhenoCam images are ostensibly available for each day, the ALMANAC model runs on a daily-timestep allowing for a consistent and simple comparison. The model, while simulating early season greenup, late season senescence, and maximum leaf area cover (via leaf area index), benefits from having actual field data for validation and improvement. The PhenoCam network benefits by having a simulation tool to expand the results to large areas with diverse soils, weather, and plant types. It has been established that for some ecosystems the use of near-surface remote sensing provides a satisfactory tool for assessing and projecting the status of vegetation. However, there is no established or routine protocol for doing so [4,11,12].

In this study, we selected diverse sites, then ran simulations in ALMANAC, and compared its leaf area index (LAI) values to color analyses results from ImageJ software using images from the PhenoCam Network. The selected sites are part of the Long-Term Agroecosystem Research (LTAR) Network, which is managed by the United States Department of Agriculture's Agricultural Research Service in partnership with local institutions. It represents a range of different agroecosystems and climatic conditions with the intention of applying experimental research findings to the sustainable intensification of US agriculture [13]. Methods from this study can be applied to other sites in the LTAR network as well as other observation networks in the PhenoCam network.

The objective of this study was to use PhenoCam data, image analysis, and Beer's law with established extinction coefficients to determine the LAI of the photograph and compare it with the LAI simulated in the ALMANAC model for diverse plant types and diverse environments. We present data from PhenoCam images analyzed in ImageJ [14] using the L*A*B* color space to determine the green leaf area, results from ALMANAC simulations run for appropriate plants using site specific weather and soil data, and finally the comparison of LAI estimated from imagery and modeled from ALMANAC. This study shows the potential when linking the ALMANAC model and the PhenoCam system. Using these combined tools, more accurate simulations can be achieved nationwide, expanding the benefit of

Table 1. A brief overview of the sites, their locations, crops [15], and soil [16]

Site name	County	State	Latitude	Longitude	Vegetation	Soil Name
Archboldpnotx	Highlands	Florida	27.1807	-81.2007	Bahiagrass (*Paspalum notatum*)	Oldsmar fine sand, 0-2% slopes
Tworfaa	Falls	Texas	31.4777	-96.8882	Maize (*Zea mays*), Alfalfa (*Medicago sativa*)	Heiden clay, 1-3% slopes
Arsmorris1	Stevens	Minnesota	45.6167	-96.1269	Maize, Soybeans (*Glycine max*)	Aazdahl-Balaton clay loams, 0-2% slopes
Arsmorris2	Stevens	Minnesota	45.6270	-96.1270	Wheat (*Triticum aestivum*)	Flom-Aazdahl-Hamerly complex, 0-2% slopes
Ibp	Doña Ana	New Mexico	32.589	-106.847	Black Grama (*Bouteloua eriopoda*)	Wink-Harrisburg association, 1-5% slopes
Jernort	Doña Ana	New Mexico	32.619	-106.788	Honey Mesquite (*Prosopis glandulosa*)	Onite-Pintura complex-Sandy, 1-5% slopes
Jerbajada	Doña Ana	New Mexico	32.5799	-106.6338	Creosote Bush (*Larrea tridentata*)	Dona Ana-Chutum complex, 1-10% slopes
Jersand	Doña Ana	New Mexico	32.515	-106.798	Creosote Bush	Onite-Pajarito association, 1-5% slopes

Table 2. Crops and their threshold metrics

Site	Crop	A*
Archboldpnotx	Bahiagrass	120
Tworfaa	Maize, Alfalfa	120
Arsmorris1	Maize, Soybeans	120
Arsmorris2	Wheat	120
Ibp	Black Grama	127
Jernort	Honey Mesquite	127
Jerbajada	Creosote Bush	140
Jersand	Creosote Bush	140

**Within the L*A*B* color space, A* was adjusted to these levels in order to best highlight the green growth within the PhenoCam images*

PhenoCams even where they are not installed, and allowing for more accurate modeling to occur.

2. MATERIAL AND METHODS

Eight sites (Table 1) were selected for their diverse locations, contrasting species, and amount of and quality of available information. Each site underwent several steps: data acquisition for images and GCC, image analysis in ImageJ, simulation in ALMANAC, then a transformation and analysis. Simulations were completed through 2019, the last full year of data.

2.1 Data Acquisition for Images and GCC

Green Chromatic Coordinate (GCC) measures green light relative to red light and blue light and can be plotted as a time series. It can be expressed as:

$$GCC = DN_G / (DN_R + DN_G + DN_B), \quad (2)$$

where DN represents digital numbers ranging from 0-255 in the red, green, and blue image bands [17]. It has been successfully used to measure phenology and gross primary productivity in diverse habitats like forests and deserts [11,15,18–20]. When using GCC to measure the health of vegetation, one operates under the assumption that healthy plants will reflect more green light than unhealthy plants [2,18]. However, it is better at controlling for varying illumination in photographs than other methods of quantifying color [17]. Although this method has its benefits, a notable limitation of using GCC includes that it cannot compensate for how much vegetation greenness varies by plant species, canopy structure, and foliar nitrogen [21]. For example, GCC has been found to be in good agreement with start-of-season and end-of-season indicators for honey mesquite, but not black grama; for both species it correlated well with canopy greenness [22]. However, [5] and [23] have found there is not a reliable direct correlation between LAI and GCC.

The PhenoCam Network serves as a repository and server for derived data such as GCC at 1- and 3-day time steps as well as the daily digital images and region of interest (ROI) mask files. The ROI is the specific area of each PhenoCam field of view over which the pixel values are summarized to compute GCC. GCC is derived for the ROI at each site at both hourly time increments and as a total daily value in the daylight hours. GCC data, photographs, and ROI files were downloaded from the PhenoCam Network's website [1]. Although multiple GCC datapoints are available for most days, GCC data was filtered by time and date to include only one measurement per day, specifically the one nearest to noon as the image analysis used in the next step needed to reduce the effect of shadows. To match the daily GCC value with LAI from a single daily image from each PhenoCam, we selected the daily image closest to noon during the first available clear day of each month during the growing season. Photographs were also used from the 15th of the month for the Minnesota sites as these had a shorter growing season and more data were needed to make the analysis more robust.

2.2 Image Analysis in ImageJ

Instead of using all daily images, only a few were needed to compare the resulting values with GCC values, and compare ImageJ values converted to LAI with ALMANAC's LAI values to see if seasonal trends were similar, thus reducing the time spent downloading and processing images. ImageJ is a java-based image analysis software which has found uses in a wide variety of fields [14]. Selected PhenoCam images were analyzed to quantify percent greenness in ImageJ based on the ROI masks for each PhenoCam to ensure the same area is analyzed in each image. This was accomplished by using the Image Menu to adjust the color threshold. The L*A*B* color space was used instead of H*S*V*, R*G*B*, or Y*U*V* to take advantage of its ability to distinguish between similar colors and its device independency [24]. Device independency ensures that the ability to identify a color by coordinates does not change with different equipment. A*, the coordinate that reflects a color's position between magenta and green, was adjusted. Different crops required different threshold metrics to accurately capture leaf area from the image as not every species will be the same shade of green (Table 2). The threshold for A* was determined visually using the photo from maximum leaf area and adjusting the value until the green leaves were selected.

Once the threshold was applied to the image, the ROI from the PhenoCam was overlaid (Image 1) to ensure the same image pixels were used in GCC and ImageJ calculations. This was done using the Edit menu, then using Select and Image to Selection to make the ROI file "zero

transparent", then overlaid it onto the image of the sites [14,25]. The Analyze Menu's Analyze Particle function was used to find Percent Area Fraction. The resulting number represents the green area within the ROI of the photo.

2.3 Simulation in ALMANAC

In ALMANAC, simulations were created using site specific weather files, soil and crop information. Data from weather stations nearest each site were used [26–31] (Table 3), and soils were obtained from NRCS WebSoilSurvey [16] (Table 1). The simulated LAI values from ALMANAC generated using default parameters indicated that changes needed to be made to the plant parameters or to the management scenario. Again, this is typical and expected when moving growth parameters from their site of origin to a new location and with different management scenarios, minor changes to the simulation will be needed as not all species were grown in the same conditions. Management dates were primarily determined by observing changes in the PhenoCam images. Such changes are documented in Table 3.

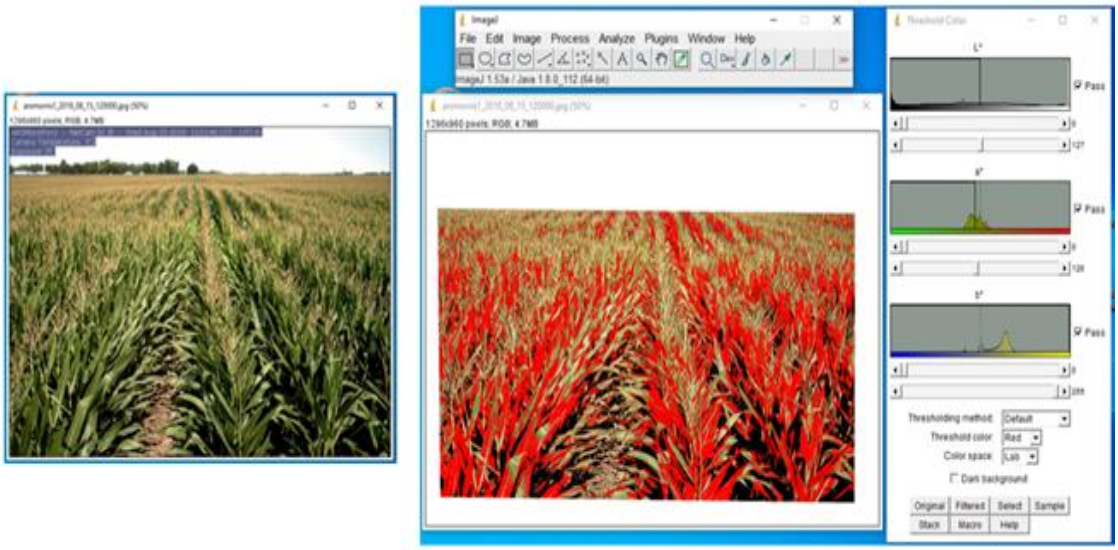

Image 1. An image acquired 8/15/2018 from arsmorris1 PhenoCam of maize growing in Minnesota (left) and then the same image (right) with the A* color threshold 0-120 and the ROI overlaid. The red shading indicates the green leaf area that will be measured and compared with the total ROI to determine green leaf area index.

Table 3. Weather data used in simulations

Site	Years	Variables	Source: Site Name
archboldpnotx	2018-2019	T, P	NOAA: USC00080236
tworfaa	2018-2019	SR, T, P, H, W	USDA-ARS: Riesel
arsmorris1	2018-2019	T, P	NOAA: USC00215638
arsmorris2	2018	T, P	NOAA: USC00215638
ibp	2015-2019	T, P, H, W	LTER: G-IBPE
jernort	2006-2019	T, P, H	NOAA and LTER: USC00294426 and M-NORT
jerbajada	2014-2019	T, P, H	NRCS SCAN: 2168
jersand	2014-2019	SR, T, P, H, W	LTER: C-SAND

**Years correspond to those used for the simulations for which we had PhenoCam imagery and weather data.*
**Weather variables are: Solar Radiation (SR), Minimum Temperature and Maximum Temperature (T), Precipitation (P), Relative Humidity (H), and Wind Speed (W).*
**The source lists where the weather data was from and the name of the site used. Four sources were used NOAA [26], LTER [27–29], NRCS SCAN [30], and USDA-ARS [31].*

Plant parameters for ALMANAC adjusted for this study consisted of those that affect leaf area index (LAI) over the growing season. Plant parameters were adjusted to match the simulated LAI values with those calculated from the PhenoCam image results. Once the crop category was set (annual warm season crop, deciduous woody species, evergreen woody species, or perennial warm season grass), the sum of degree days (PHU) for a year from planting or greenup to maturity was set (using the already established base and optimum temperatures for the plant species). The potential leaf area index (DMLA) was the first parameter adjusted. The fraction of the growing season (in degree days) when maximum LAI occurred (DLAI) was adjusted next. Two parameters for the "S" curve for leaf area index increase are DLAP1 and DLAP2. These are each two-part parameters. The number to the left of the decimal is the fraction of the season and the number to the right of the decimal is the fraction of maximum LAI. Thus, if DLAP1 and DLAP2 are 10.05 and 50.95, plants reach 5% of potential LAI at 10% of seasonal degree days (PHU) and 95% of potential at 50% of PHU. Two more two-part parameters are PPL1 and PPL2. PPL1 is plant population (plants/m^2) at a lower density and the number after the decimal is the fraction of maximum LAI reached at that density. The same goes for PPL2 but it is at a higher density. A parameter important for multi-year runs with perennials is the CHTYR, that is the number of years until plants reach their potential LAI. The rate of leaf area decline late in the season (RLAD) can be linear, or curvilinear depending on whether RLAD is 1.0, or above or below 1.0. Finally, a dormancy parameter (DORMNT) defines how perennial plants go dormant as the photoperiod approaches the minimum for the year.

Adjustment of plant parameters followed a logical sequence. First, the height of the LAI curve from the PhenoCam results was matched by adjusting the potential LAI in ALMANAC (DMLA). Secondly, the timing for when maximum LAI is during the season (DLAI, fraction of the season's PHU) was adjusted to match the ALMANAC simulated values with those from the PhenoCam

Image 2. Image from archboldpnotx PhenoCam taken on July 1st, 2017

Table 4. ALMANAC plant parameter changes made based on PhenoCam inputs

Crop	Site	DMLA	DLAI	DLAP1	DLAP2	CHTYR	RLAD	DORMNT
Alfalfa	Default	-	-	15.01	50.95	-	-	-
	tworfaa*	-	-	55.18	86.83	-	-	-
Bahiagrass	Default	2	0.7	22.12	54.62	0	-	-
	Archboldpnotx	1.25	0.25	1.13	11.76	1	-	-
Black Grama	Default	1.5	0.35	-	30.07	0	0.1	-
	lbp	2	0.53	-	40.72	1	0.9	-
Creosote Bush	Default	2.75	0.93	41.88	92.98	-	-	0
	jerbajada*	1.2	0.86	2.7	49.86	-	-	0.75
	jersand*	1.2	0.86	2.7	49.86	-	-	0.75
Honey Mesquite	Default	4	-	-	-	0	-	-
	jernort*	1	-	-	-	15	-	-
Maize	Default	6	0.5	-	50.95	-	0.75	-
	arsmorris1	3	0.52	-	35.82	-	0.75	-
	Tworfaa	-	-	-	-	-	1	-
Soybeans	Default	10	0.8	-	50.92	-	1	-
	arsmorris1	3.8	0.73	-	61.8	-	0.75	-
Wheat	Default	5	0.6	31.07	57.95	-	-	-
	arsmorris2	5.3	0.47	26.19	42.67	-	-	-

** Dashes represent that no change was made to the default ALMANAC plant parameter.*

** This site had an additional minor parameter changed which may include CLAIYR, DMPHT, IDC, PPL1, PPL2, or TG.*

results. Next, to get the buildup of LAI prior to DLAI, DLAP1 and DLAP2 were adjusted to get closer agreement between ALMANAC and PhenoCam results. The rate of decline of LAI in the later part of the season was matched by adjusting RLAD in ALMANAC. Finally, for creosote bush only, we adjusted the length of the dormant period in the winter (DORMNT) to match ALMANAC output with the PhenoCam results. See Table 4 and the site details for specific changes.

The archboldpnotx site is a field that is sometimes grazed but was not grazed during the period of the measurements within the Archbold Biological Station in Florida. Bahiagrass was simulated in 2018 and 2019. While bahiagrass is a perennial, and has been simulated as such within ALMANAC in Texas [32], challenges with simulating its dormancy in this subtropical area in Florida were handled by simulating each year of grass growth separately. For the simulations, bahiagrass was planted on April 1 2018 and 2019, with a PHU of 3000, and a plant population density (POP) of 50. During both years bahiagrass was hay harvested and killed on December 1. Although the field had been growing there before PhenoCam data was available and grazed prior to the simulation years, ALMANAC needed this management scenario to mimic the natural life history of bahiagrass. See Table 4 for plant parameter refinements from the default values.

At the tworfaa site in central Texas, maize and alfalfa were rotated for two years in 2018 and 2019. In 2018 maize was planted on February 15, with PHU of 1700 and POP of 7, and then harvested on July 25. Alfalfa was planted September 26, with PHU of 1590 and POP of 22, and then hay harvested and killed on March 18, 2019. Maize was planted again on March 27, 2019, with PHU of 1700 and POP of 4, and then harvested on August 26. Alfalfa was planted October 28, with PHU of 1590 and POP of 22. For TWORFAA there was not camera data available for the maize planting in 2018, so assumptions were made based off typical practices in this region. Lower POP was used for maize in 2019 based on the gaps seen between plants in the PhenoCam images. Plant parameter refinements are listed in Table 4 with one addition, alfalfa's IDC (crop category) was changed from 2 (cold season annual legume) to 5 (cold season annual).

Image 3. Image taken by PhenoCam of tworfaa on June 1st, 2018

Image 4. Image taken by PhenoCam of arsmorris1 on September 1st, 2018

Image 5. Image taken by PhenoCam of arsmorris2 on July 1st, 2018

At the arsmorris1 site, viewed from the south tower of the ARS Morris LTAR site in Minnesota, maize and soybeans were rotated for two years in 2018 and 2019. During 2018, maize was planted on April 10 with a PHU of 1470 and a POP of 7, and then harvested on September 16. During 2019, soybeans were planted on June 10 with a PHU of 1120 and a POP of 50, and then harvested on October 6 of the same year. See Table 4 for plant parameter refinements from the default values.

At the arsmorris2 site, viewed from the north tower of the ARS Morris LTAR site in Minnesota, wheat was simulated in 2018. Wheat was planted on April 1 with 1800 PHU and 125 POP, then harvested on September 30 of the same year. See Table 4 for plant parameter refinements from the default values.

At the ibp site within Jornada Experimental Range in New Mexico, black grama was simulated from 2015 to 2019. In 2015, black grama was initially planted on April 1, with PHU of 2020 and POP of 2.2. Each year a harvest operation was set to remove 90% of the above ground black grama on December 31. Although the field is unmanaged and had been growing there before PhenoCam data was available, ALMANAC needed this management scenario to simulate the natural life history of black grama. See Table 4 for plant parameter refinements from the default values.

At the jernort site within Jornada Experimental Range in New Mexico, honey mesquite was simulated from 2006 to 2019. The model had to begin in 2006 to obtain adequate growth before the years of analysis (2015-2019). This is often done in modeling simulations for woody species. Jernort had two weather sources (Table 3). 2006-2014 temperature and precipitation were from NOAA. 2015-2019 temperature, precipitation, and humidity were from LTER. LTER site was at the field location and occurred during the period of analysis, but data precluding the station was needed. For the simulations, mesquite was planted on January 1, 2006 with PHU of 2530 and POP of 10. For all years, 32% of above ground biomass was cut and allowed to drop to the ground on June 22, July 20, and August 17. Although the field is unmanaged and had been growing there before PhenoCam data was available, ALMANAC needed this

Image 6. Image taken by PhenoCam of ibp on October 1st, 2015

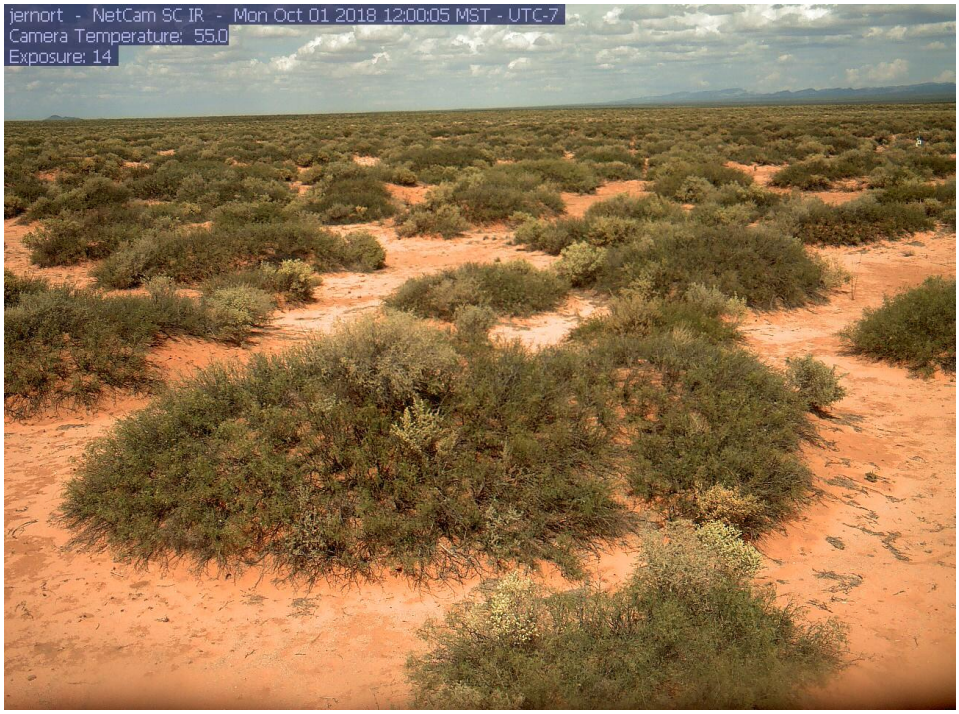

Image 7. Image taken by PhenoCam of jernort on October 1st, 2018

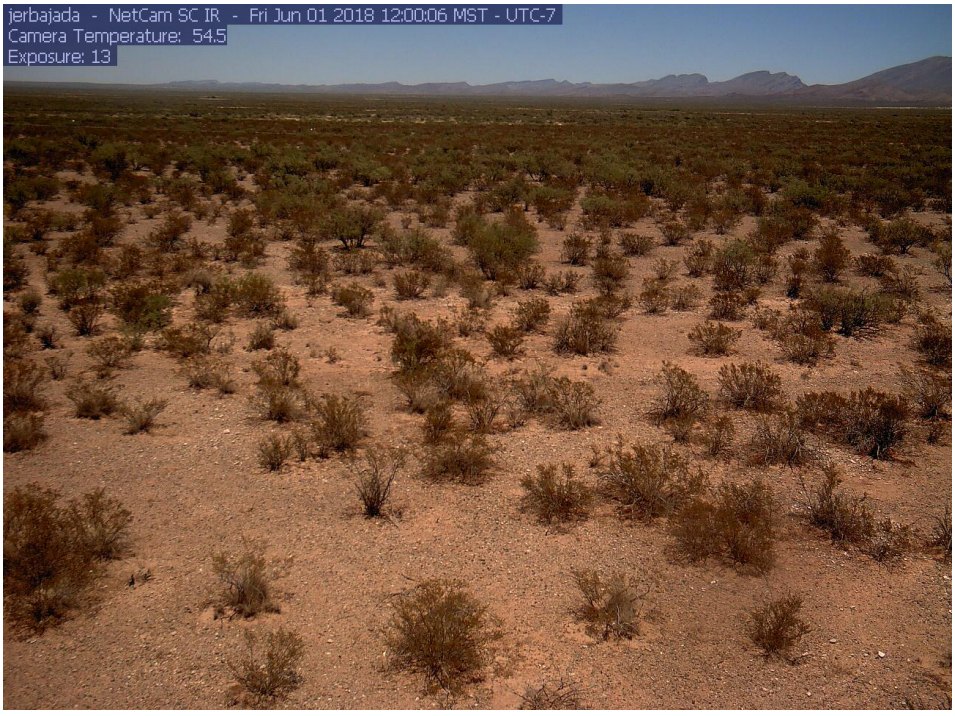

Image 8. Image taken by PhenoCam of jerbajada on June 1st, 2018

management scenario to simulate the natural life history of honey mesquite. Plant parameter deviations from the default values are listed in Table 4 along with these additions: PPL1 was

changed from 1.98 to 1.14, PPL2 was changed from 2.99 to 5.95, IDC was changed from 7 (for evergreen plants) to 8 (for deciduous plants), CLAIYR (year to maximum LAI) was changed from 8 to 15, and DMPHT (multi-year perennial parameter meaning minimum grams of biomass per meter of height) was changed from 0.75 to 0.

The jerbajada site within Jornada Experimental Range in New Mexico, creosote bush was simulated from 2014 to 2019. The first year of the simulation was used to reach the amount of growth reflected in the images and was not used in the analysis. In 2014, creosote bush was planted on January 1 with a PHU of 2700 and a POP of 23. Then the crop was sequentially harvested every two weeks, beginning August 26th to November 31st, to simulate late season leaf drop. The override of harvest index (ORHI) was set at 0.04, and the harvest efficiency (HE) was set at 0.01. These two parameter changes implement a 4% harvest of the aboveground biomass being dropped on the ground for each harvest operation. Although the field is unmanaged and had been growing there before PhenoCam data was available, ALMANAC needed this management scenario to simulate the natural life history of creosote bush. In order to simulate a similar creosote bush, we used parameters from [33] for a small bush, which recommended PPL1 20.01, and PPL2 35.03. To customize the crop parameters further we changed PPL1 to 20.2, PPL2 to 35.99, TG (base temperature for plant growth) from 15 to 10, and the remaining changes are listed in Table 4.

At the jersand site in New Mexico, creosote bush was simulated from 2014 to 2019. The first year of the simulation was not used in the analysis as this period allowed the woody plant a closer approximation to the growth reflected in the images. Parameters and management were the same as listed above in the jerbajada site except POP was set to 25. This minor deviation in POP was implemented after comparing the ROI for the two sites both visually and with the GCC converted to LAI.

2.4 Data Analyses

To reiterate, GCC does not equal LAI and therefore cannot be directly compared with ALMANAC. As such, ImageJ is used to analyze the photos so that GCC can be converted to LAI

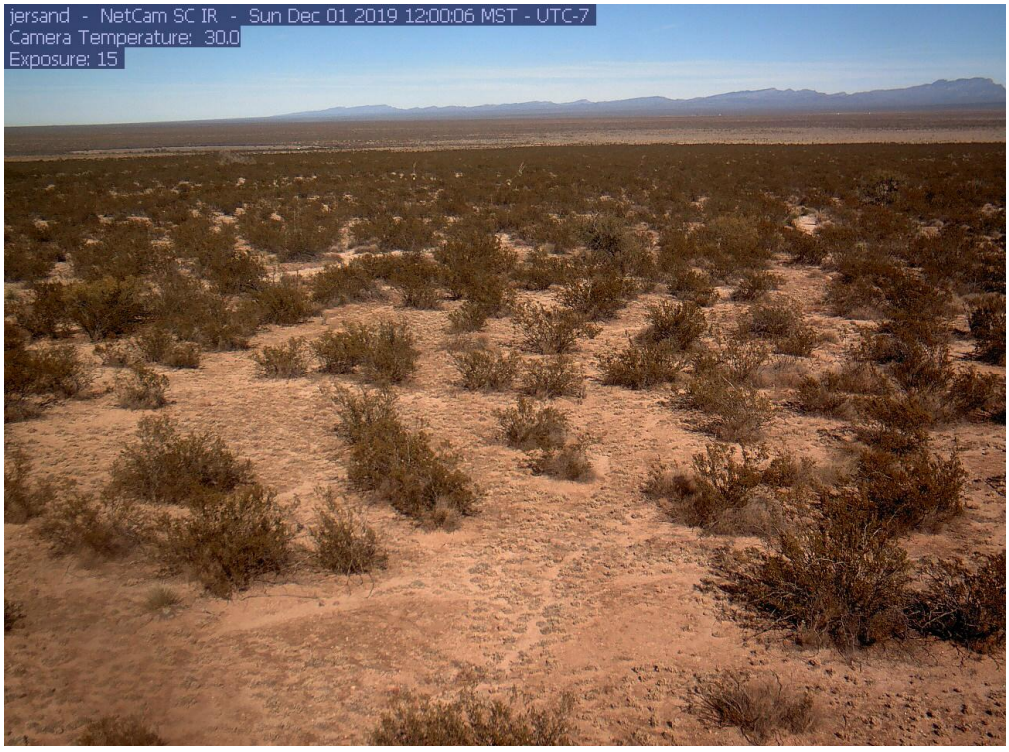

Image 9. Image taken by PhenoCam of jersand on December 1st, 2019

on a site by site basis. GCC is used because this data is reported daily, so once conversions are done for a few days with ImageJ, time and labor is saved by not doing image analysis for everyday of the year and instead using the conversion for GCC. This is done by initially comparing PhenoCam's GCC to ImageJ's Percent Area Fraction of green. At each site the PhenoCam GCC and the ImageJ Percent Area Fraction of green areas were transformed and plotted as a regression (Fig. 1). The GCC transformation (Equation 3) ensured the lowest recorded GCC would be treated as the minimum value and the range from minimum to maximum was taken into account. This was important on a site by site basis as the GCC values differ very little. For example, at archboldpnotx the GCC min and max were 0.330 and 0.474 respectively. The Percent Area Fraction transformation (Equation 4) allowed for a zero to one scale for the regression. This regression shows how closely our image analysis corresponded to the PhenoCam.

Transformed GCC = (GCC – Minimum GCC) / (Maximum GCC – Minimum GCC) (3)

Transformed %area fraction = (%area fraction) * 0.01 (4)

Transformed ImageJ results were converted with Beer's law to LAI to be plotted against ALMANAC's simulated LAI values (top graphs Figs. 2-9). Only a few ImageJ points were needed to see that LAI results were trending in the same direction. This cut down on image processing time as opposed to processing images for every day of the year. With ImageJ's Percent Area Fraction quantifying how much of the photo is green, this corresponded to actively photosynthesizing leaf area. As such, the values can be converted to LAI using Beer's law and then compared with ALMANAC. If the ALMANAC simulations appeared to follow the infrequent image analysis, we proceeded with the regression of ImageJ and GCC (Fig. 1). This bridged the gap between GCC values and derived values for Percent Area Fraction The resulting regression was then used to convert GCC to LAI, by inputting transformed GCC into the regression equation (converting it to ImageJ greenness) (Equation 5), and then that result into Beer's law (converting it to LAI) (Equation 6). For Beer's law, the plant extinction coefficient (k) used was listed in ALMANAC and was different for each plant species. This working LAI value was compared with ALMANAC's simulated LAI (bottom graphs Figs. 2-9), and further ALMANAC refinements were implemented as necessary.

Converted GCC = (MAX (regression equation with Transformed GCC as x), 0) (5)

LAI of PhenoCam = (ln (1 - Converted GCC)) / (plant extinction coefficient) (6)

3. RESULTS AND DISCUSSION

ImageJ versus GCC regressions R^2 values were all greater than 0.5 except for the IBP site (0.39). Individual site regressions along with the equations used in later calculations are shown in Fig. 1, while R^2 values for species are displayed more clearly in Table 5. Judging by the R^2, soybeans (0.84), mesquite (0.76), and maize (0.75) produced the most successful match between the GCC and PhenoCam data (Table 5). Black grama and creosote bush had the weakest correlation with R^2 of 0.39 and 0.53 respectively.

Table 5. Average R^2 values sorted by crop

Crop	R2 Average	Crop	R2 Average
Alfalfa	0.66	Maize	0.75
Bahiagrass	0.66	Mesquite	0.76
Black Grama	0.39	Soybeans	0.84
Creosote Bush	0.53	Wheat	0.73

The following results are organized by site with Figs. 2-9 indicating (top graphs) the LAI of ALMANAC vs LAI of Percent Area (green) from ImageJ, and (bottom graphs) the LAI of ALMANAC vs LAI of converted GCC from PhenoCams.

3.1 ARCHBOLDPNOTX, FL: BAHIA-GRASS

The ImageJ versus GCC regression has an R^2 of 0.65 (Fig. 1). The ALMANAC simulations with the adjusted parameters much more realistically simulated the PhenoCam LAI values (Fig. 2). The ALMANAC LAI compares well with the GCC converted to LAI. ALMANAC follows the seasonality of the bahiagrass but does not reach as high LAI peak as the GCC LAI.

3.2 TWORFAA, TX: MAIZE + ALFALFA

The ImageJ versus GCC regression has an R^2 of 0.89 for maize and 0.66 for alfalfa (Fig. 1). Once

again, the ALMANAC simulated LAI values with the adjusted parameters was superior to the simulated values with the default parameters (Fig. 3). The ALMANAC LAI in the first and third years compares well with the GCC converted to LAI. ALMANAC is under predicting maize in 2018, but is within reason. The comparison differs slightly towards the end of the alfalfa growing season, with ALMANAC plateauing and GCC increasing.

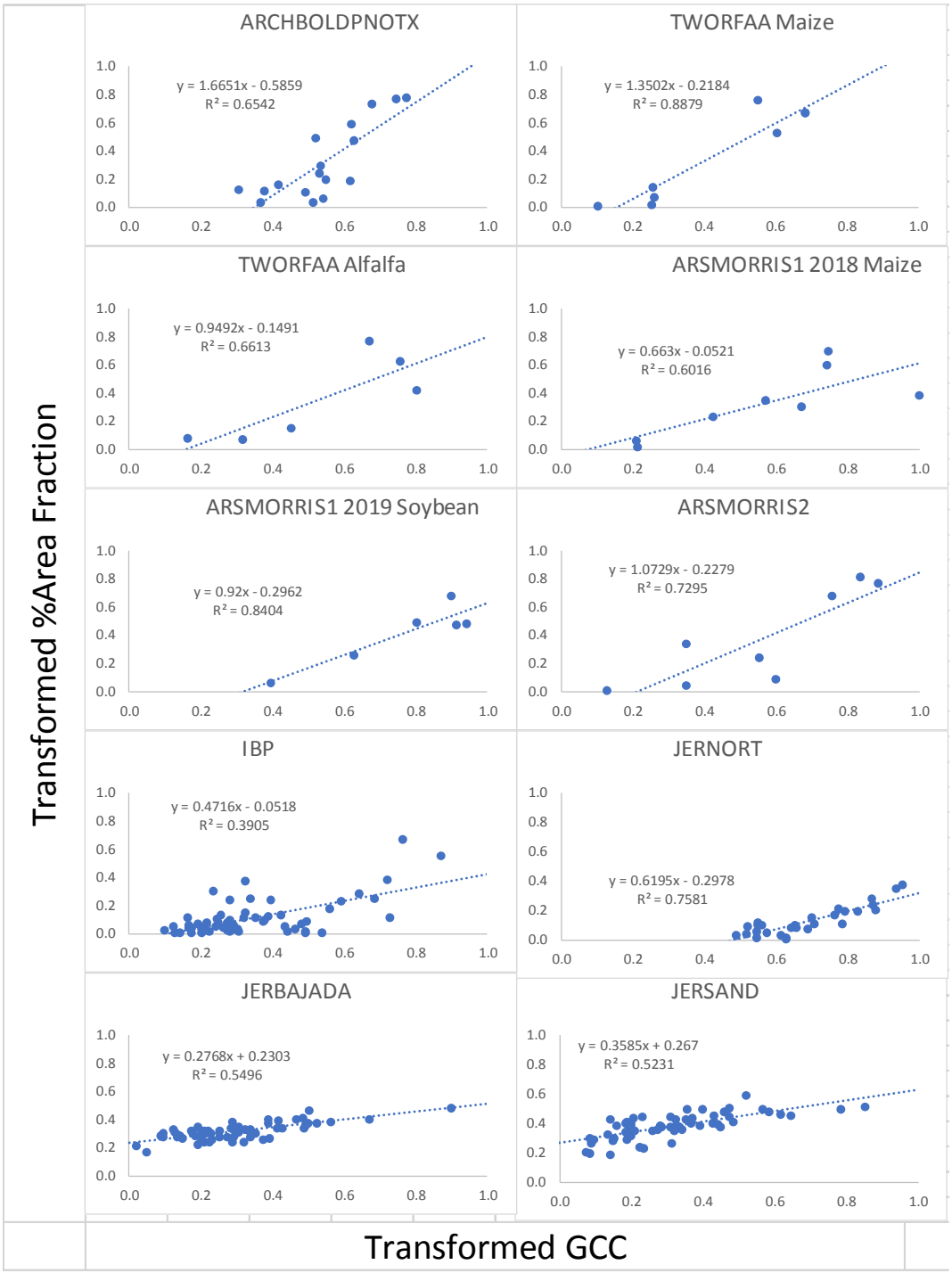

Fig. 1. Visualizations of the regressions for each crop at each site

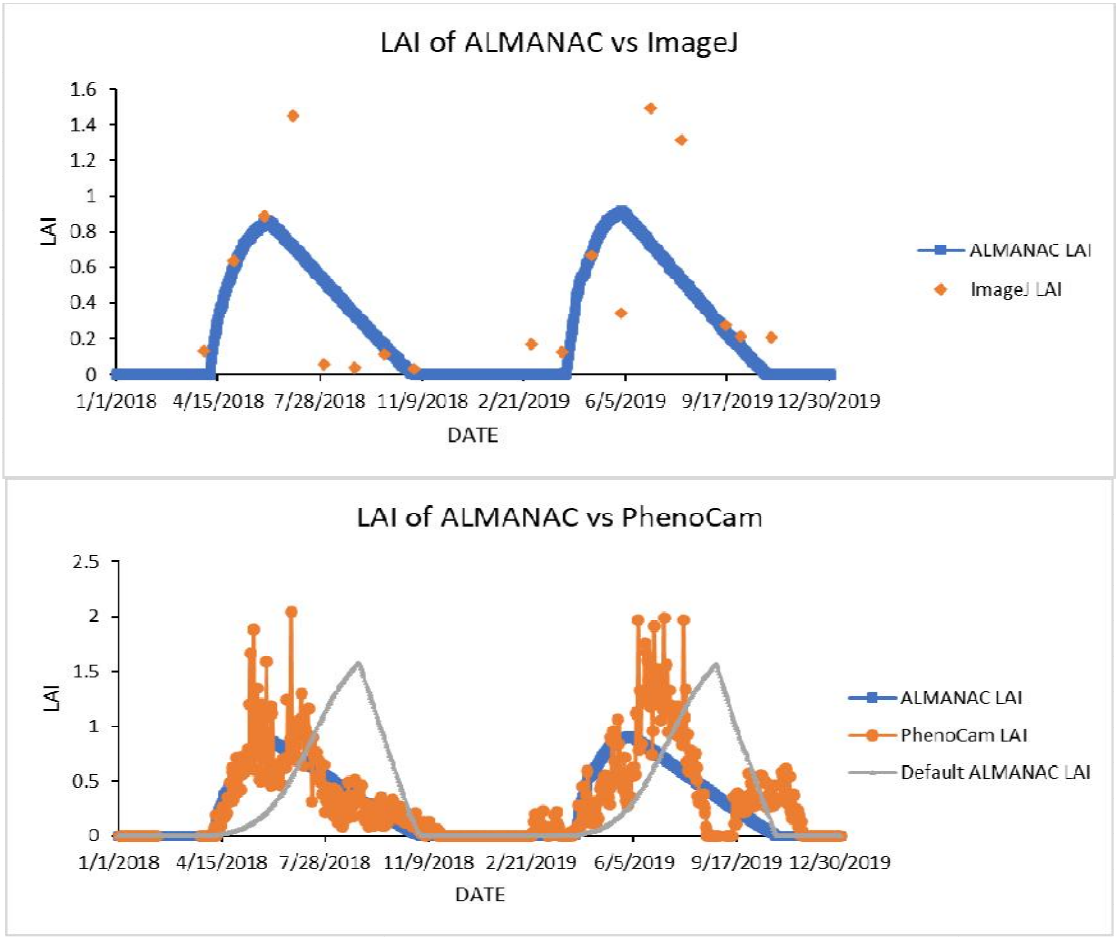

Fig. 2. Graphs of bahiagrass from archboldpnotx comparing the LAI from ALMANAC with image analyses results (top) and then the LAI from ALMANAC with the transformed GCC from the PhenoCam website and the LAI from ALMANAC using default plant parameters (bottom)

3.3 ARSMORRIS1, MN: MAIZE + SOYBEAN

The ImageJ versus GCC regression has an R^2 of 0.6 for maize and 0.84 for soybeans (Fig. 1). The adjusted parameters greatly improve ALMANAC's values (Fig. 4). The ALMANAC LAI compares well with the GCC converted to LAI but is slightly overpredicting maize's peak LAI values.

3.4 ARSMORRIS2, MN: WHEAT

The ImageJ versus GCC regression has an R^2 of 0.73 (Fig. 1). Both the default parameters and the adjusted parameters result in reasonable values for ALMANAC LAI (Fig. 5). The ALMANAC LAI compares well with the GCC converted to LAI. The PhenoCam records a fall growth of weeds that ALMANAC doesn't show. At the end of the year, the image analysis picked up on winter weeds growing in the fallow field, while ALMANAC did not. ALMANAC can capture this additional growth if a cool season annual is planted. Since focus was put on the two crops growing, the authors choose not to amend the simulation.

3.5 IBP, NM: BLACK GRAMA

The ImageJ versus GCC regression has an R^2 of 0.39 (Fig. 1). The ALMANAC LAI values with the adjusted parameters shows only modest improvement as compared with the values with the default parameters (Fig. 6). The ALMANAC LAI with adjusted parameters compares fairly well with the GCC converted to LAI. In 2015 they were very close, 2016-2018 ALMANAC peaked early but with similar values. However, in 2019 ALMANAC is underestimating the LAI.

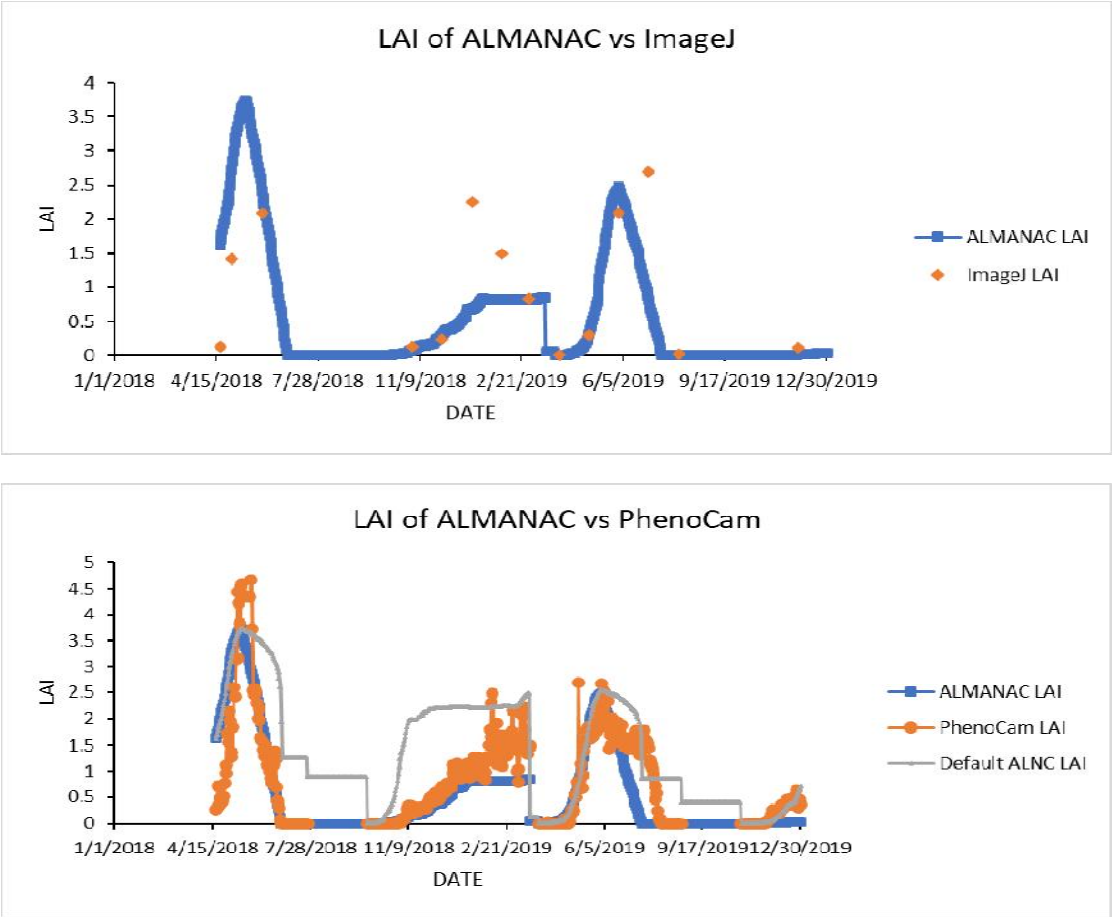

Fig. 3. Graphs of maize followed by alfalfa from tworfaa comparing the LAI from ALMANAC with image analyses results (top) and then the LAI from ALMANAC with the transformed GCC from the PhenoCam website and the LAI from ALMANAC using default plant parameters (bottom)

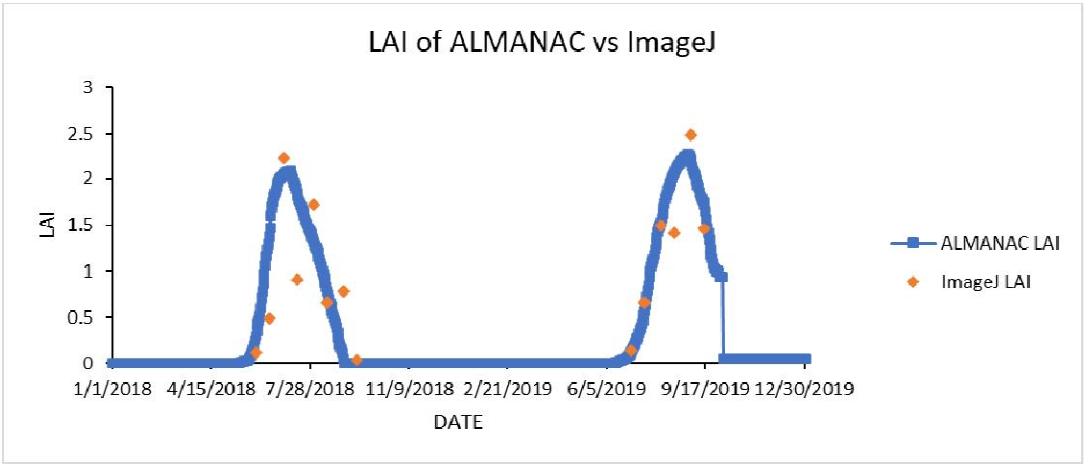

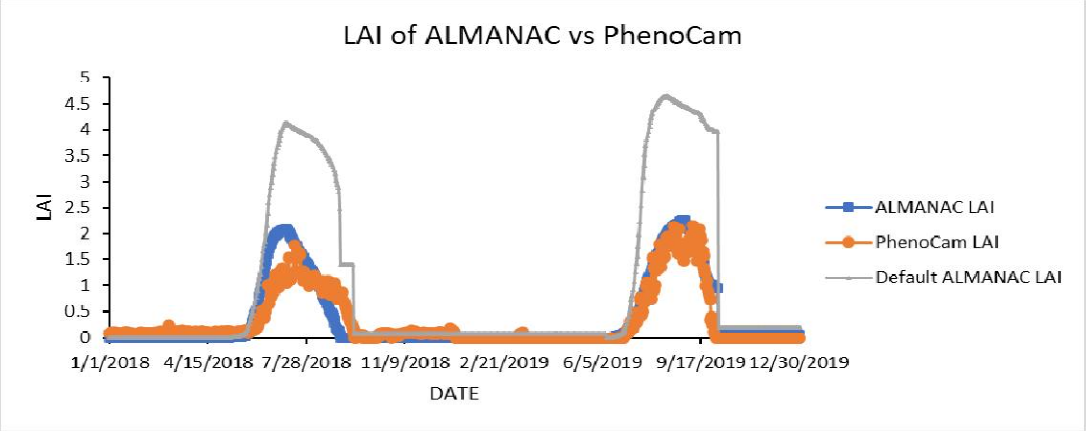

Fig 4. Graphs of maize followed by soybean from arsmorris1 comparing the LAI from ALMANAC with image analyses results (top) and then the LAI from ALMANAC with the transformed GCC from the PhenoCam website and the LAI from ALMANAC using default plant parameters (bottom)

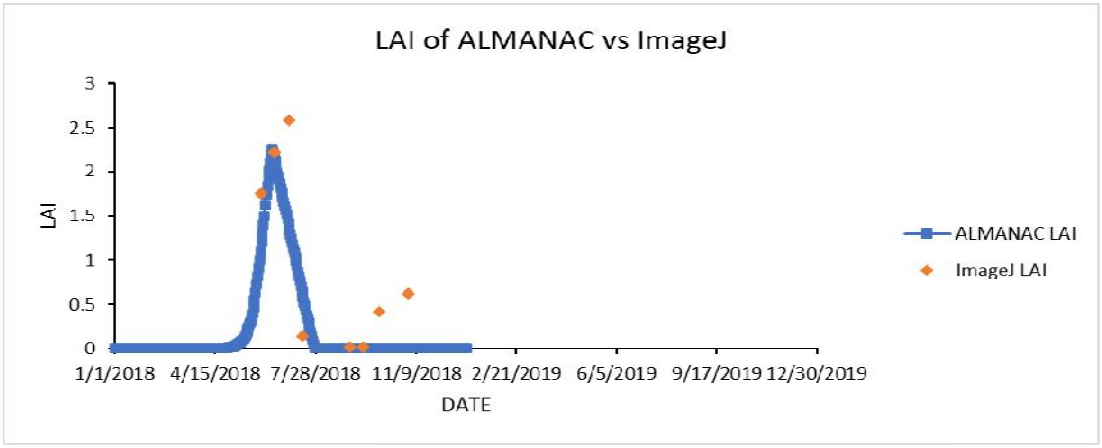

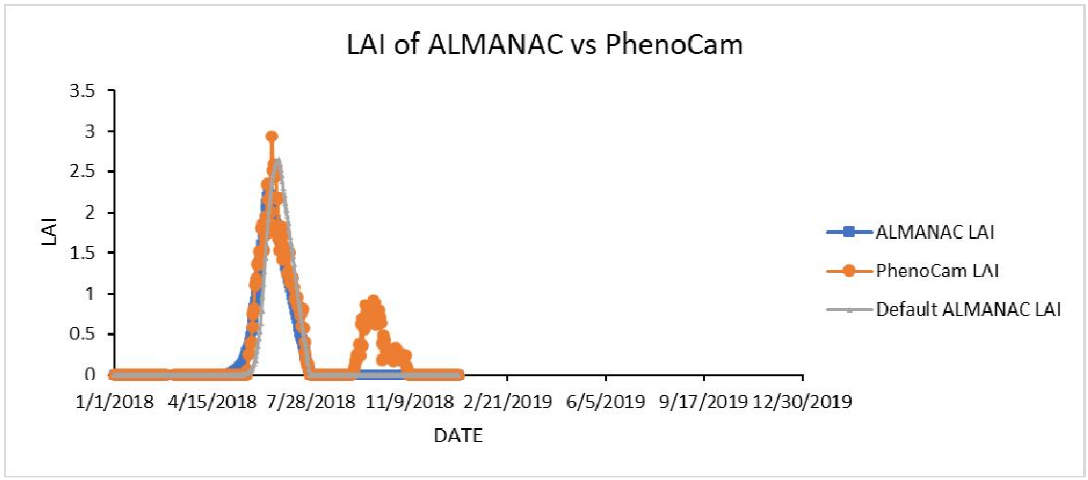

Fig. 5. Graphs of wheat from arsmorris2 comparing the LAI from ALMANAC with image analyses results (top) and then the LAI from ALMANAC with the transformed GCC from the PhenoCam website and the LAI from ALMANAC using default plant parameters (bottom).

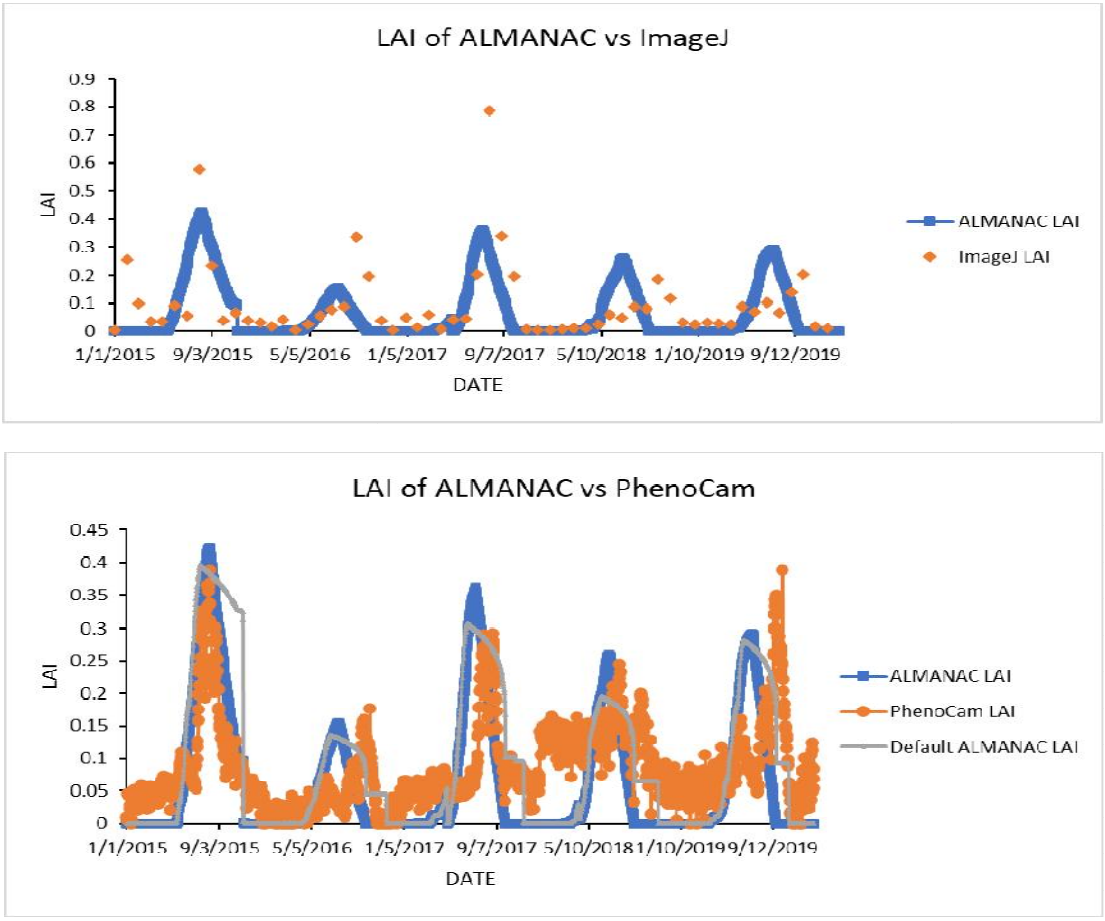

Fig. 6. Graphs of black grama from ibp comparing the LAI from ALMANAC with image analyses results (top) and then the LAI from ALMANAC with the transformed GCC from the PhenoCam website and the LAI from ALMANAC using default plant parameters (bottom)

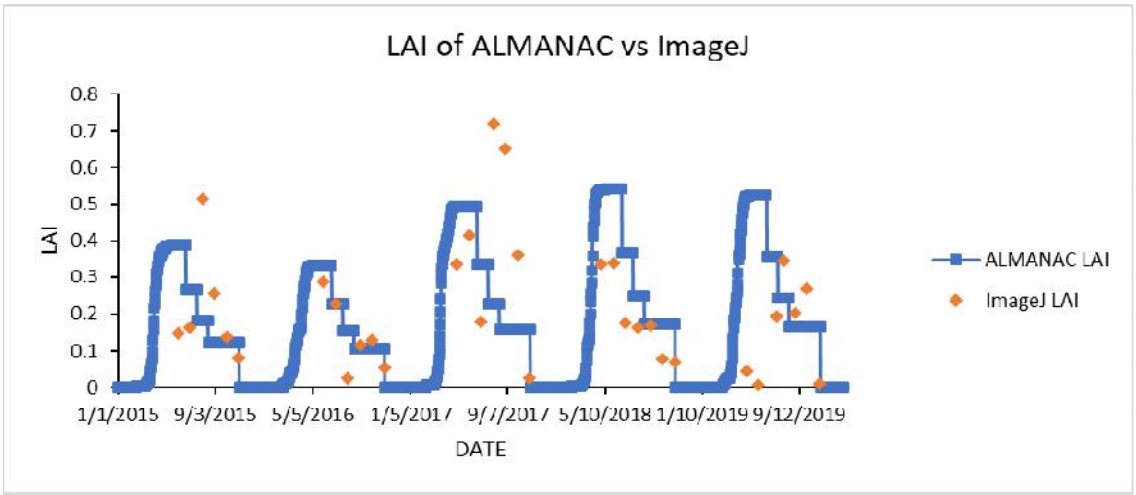

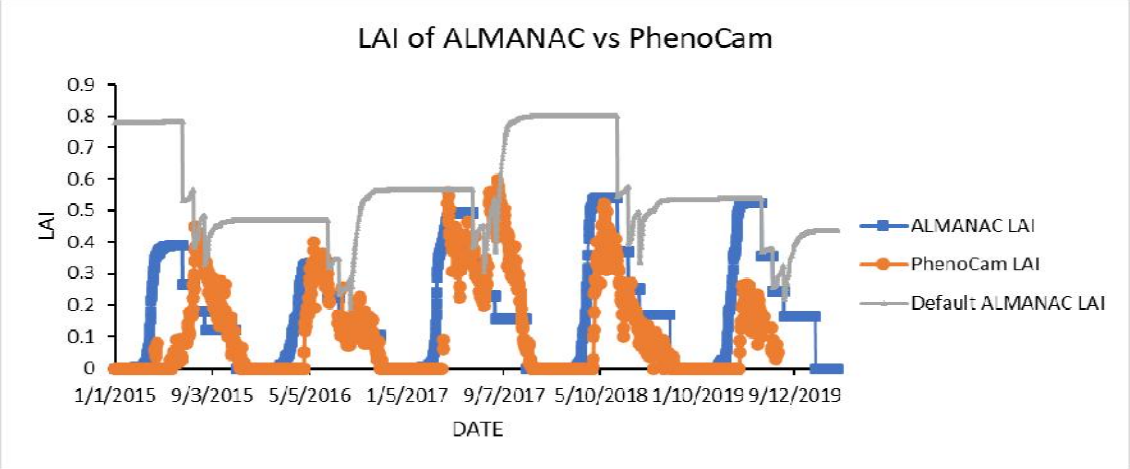

Fig. 7. Graphs of honey mesquite from jernort comparing the LAI from ALMANAC with image analyses results (top) and then the LAI from ALMANAC with the transformed GCC from the PhenoCam website and the LAI from ALMANAC using default plant parameters (bottom)

3.6 JERNORT, NM: HONEY MESQUITE

The ImageJ versus GCC regression has an R^2 of 0.76 (Fig. 1). The ALMANAC LAI values with the adjusted parameters are much improved as compared with the default values (Fig. 7). The ALMANAC LAI with adjusted parameters compares fairly well with the GCC converted to LAI. 2015 ALMANAC peaked early but with similar values, and in 2019 ALMANAC is overestimating the LAI.

3.7 JERBAJADA, NM: CREOSOTE BUSH

The ImageJ versus GCC regression has an R^2 of 0.55 (Fig. 1). The ALMANAC LAI with adjusted parameters compares very well with the GCC converted to LAI (Fig. 8). ALMANAC underestimates the LAI at only two points in 2017 and 2019.

3.8 JERSAND, NM: CREOSOTE BUSH

The ImageJ versus GCC regression has an R^2 of 0.52 (Fig. 1). The ALMANAC LAI with adjusted parameters compares well with the GCC converted to LAI (Fig. 9). ALMANAC is not capturing the extreme fluctuations as well and models more consistent LAI plateaus throughout the season.

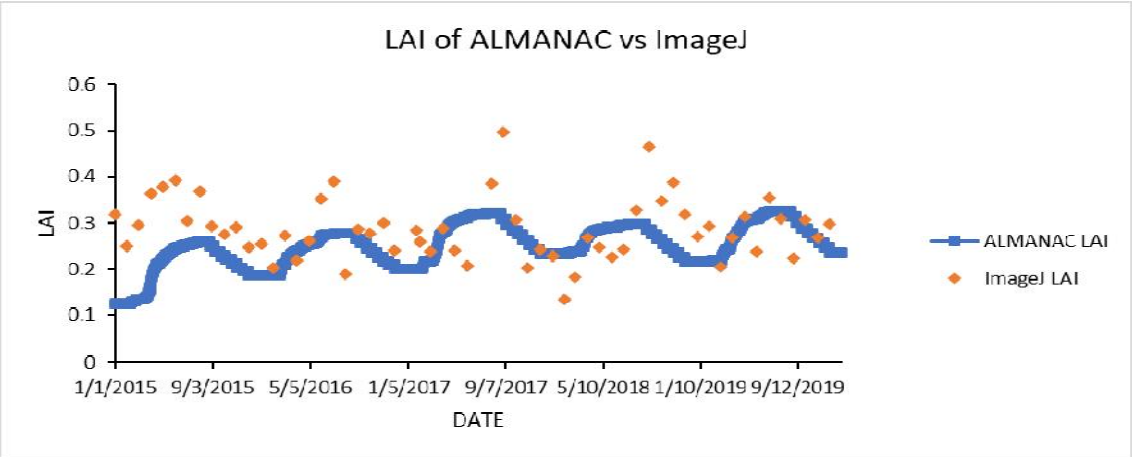

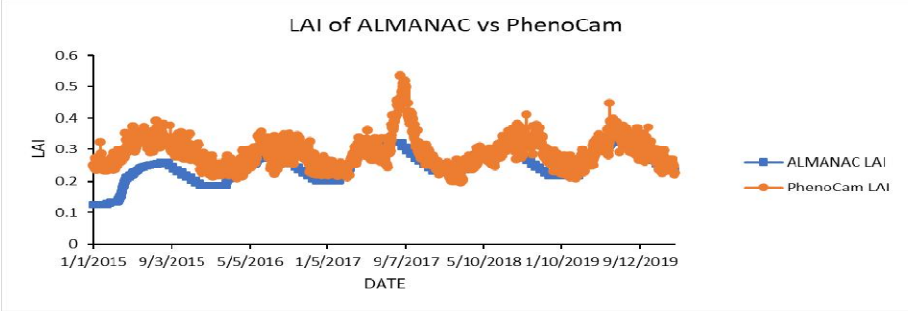

Fig. 8. Graphs of creosote bush from jerbajada comparing the LAI from ALMANAC with image analyses results (top) and then the LAI from ALMANAC with the transformed GCC from the PhenoCam website (bottom). The LAI values from ALMANAC using default plant parameters were not shown for this site due to simulation errors when they were used

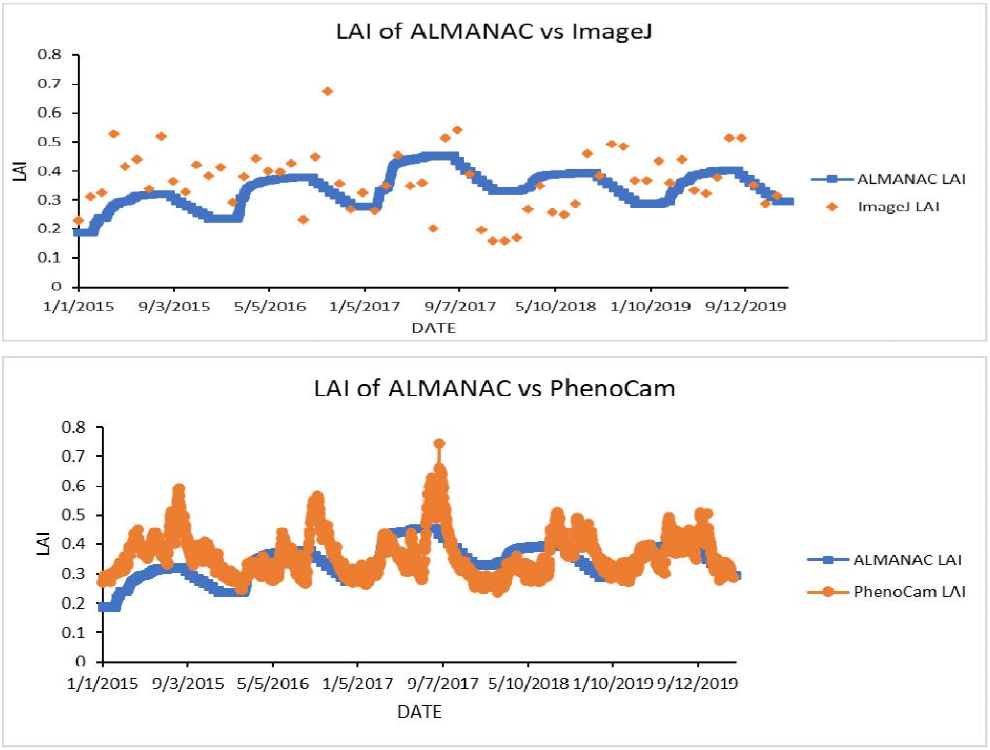

Fig. 9. Graphs of creosote bush from jersand comparing the LAI from ALMANAC with image analyses results (top) and then the LAI from ALMANAC with the transformed GCC from the PhenoCam website (bottom). The LAI values from ALMANAC using default plant parameters were not shown for this site due to simulation errors when they were used

4. DISCUSSION

We found that near surface remote sensing with PhenoCams can be used with ALMANAC simulations, Beer's Law, and L*A*B* image analysis to mimic or correlate plant growth and senescence. The ALMANAC model can be validated and improved with information from PhenoCams. For example, at many of the sites, management activities were not reported, but could be derived based on the photographs, as could senescence. This advancement provides benefits as it elaborates on ways to utilize previously established uses for digital camera technology for studies on plant phenology. For example, true color cameras have been established as more effective than infrared cameras for monitoring plant condition [17].

Other studies have applied PhenoCams to questions involving plant cover, flower count, and biomass, among others [34].

Each site provided unique challenges and insight into developing this analysis technique. For example, Minnesota's long winters led us to limit image analyses to the growing season, but fewer data points ultimately led to the decision to include more frequent image analyses. Winter weeds were not projected with our models but showed up on the GCC measurements and image analyses in Minnesota. Also, the highly variable weather of New Mexico meant we needed customized, hyper-localized weather data. Other PhenoCam sites were considered but deemed unsuitable for this first attempt due to grazing livestock or missing data; these could be other obstacles to overcome in the future.

Furthermore, the GCC data's ambiguity provided more challenges. PhenoCams are not calibrated images. The GCC reported by the PhenoCam Network only varied by 0.144 at most, so adjustments had to be made by site as to what appropriate values to use for maximum greenness and as a baseline for zero greenness or least green in the case of evergreen species. In addition, PhenoCams are subject to some atmospheric conditions that can alter the color channel brightness [34]). Due to the variations in color photos and the color variations among plant species, ImageJ greenness values were also altered to each specific plant species. This makes scaling the project up to include more sites a challenge, but it is attainable now that procedures have been established. Choosing a single image per day could also create noisy data if lighting is poor, whereas using the GCC values compiled from an entire day may reduce this by accounting for more lighting variations. Sonnentag et al. [20] recommended the use of the 90th percentile gcc value for a 3-day period, available online as GCC_90. However, using the compiled GCC value would not make a good comparison with ImageJ analysis.

In a 2020 study, Aasen et al [23] determined there was not a clear correlation between GCC and LAI however, they were able to track LAI development using the PhenoCams. While we agree there is no universal GCC and LAI relationship, our methods adapted to each site and species do allow for LAI to be determined using PhenoCams. The study would be improved by using our methods with a field experiment to determine LAI error. However, the LAI we report is already within the expected range for the plants listed in this study.

These results indicate that PhenoCam imagery can be used to improve process-based models such as ALMANAC in diverse environments. Using PhenoCams to take a picture, then image analysis to determine greenness, then Beer's law to determine LAI we compare photo LAI with model LAI. This results in a reasonable match between LAI values, therefore the other outputs from ALMANAC, such as yield, can be used. =. Using the photos saves Ftime, travel, and labor to directly measure plants when the pictures provide enough information to amend current parameters. This new approach will expand on already ground-truthed parameters by allowing photo truth for validation of new sites This research shows promise for other areas of remote sensing, agroecology, and environmental sciences where process based models are valuable tools for technology transfer. Future applications of this knowledge may include improving models other than ALMANAC or using other types of sensors with a similar protocol.

The Environmental Policy Integrated Climate Model (EPIC) has already been supported with remote sensing imagery in a 2020 study from [35]. They used data acquired from Moderate Resolution Imaging Spectroradiometer (MODIS) to assess if modelled LAI to support air quality models for retroactive and future meteorological assessments. They found that EPIC LAI simulations and MODIS LAI collections "compared favorably", although some data collections were more successful than others [35]. This shows that data from simulations, particularly LAI, can be used to supplement other remote sensing projects. On the other hand, the USDA's Forest Service have used PhenoCam data to validate a new remote sensing project, called Phenomap [36]. It is a weekly assessment of land surface "greenness" using Normalized Differential Vegetation Index (NDVI) data derived from MODIS satellite data. In order to validate their data, they used GCC_90 data from 54 non-agricultural sites and found that PhenoCams could be used to validate their satellite data but with varying reliability depending on biome. For example, Pearson's R values for open and closed needle leaf forests (four and two respectively) were low compared to deciduous forests and grasslands (fifteen and sixteen respectively). Using data collected from different perspectives illuminated the distinct advantages of near-surface and satellite remote sensing

data. Notably, they found that the NDVI data was noisier than GCC_90 data acquired from PhenoCams and, in deciduous ecosystems, NDVI lagged behind during greenup and senescence [36].

For LTAR sites with available eddy covariance data, a similar concept could be applied to identify a possible relationship between atmospheric conditions, observed plant growth, and simulated plant growth. Since sites were utilized only if they were not grazed, had GCC in a reasonable range, and were in different environments there is a lot of room for expansion. The impact of this research can be increased as the methods are refined further.

5. CONCLUSION

Our goal was to find if ALMANAC simulations, in conjunction with Beer's Law, image analysis, and data provided by the PhenoCam network could be used to simulate phenology of vegetation. By using remote sensing to validate models, not only will the models themselves be more precise, land managers and researchers would benefit from more accurate and timely knowledge of plant growth and senescence. Ultimately each site and its plant species were unique, and therefore required custom parameters and yielded results with varying precision. Although there are surely improvements to be made upon this methodology in the future, each site's simulation was improved by incorporating information from the PhenoCams. The knowledge and techniques gained during this study can be scaled up, applied to new sites in other regions, validated with different modelling software, or used with different simulated data. Continuing to hone these skills will provide more knowledge and awareness of vegetation growth in a changing world.

ACKNOWLEDGMENTS

We thank our many collaborators, including site PIs and technicians, for their efforts in support of PhenoCam. The development of PhenoCam has been funded by the Northeastern States Research Cooperative, NSF's Mac-rosystems Biology program (awards EF-1065029 and EF-1702697), and DOE's Regional and Global Climate Modeling program (award DE-SC0016011). We acknowledge additional support from the US National Park Service Inventory and Monitoring Program and the USA National Phenology Network (grant number G10AP00129 from the United States Geological Survey), and from the USA National Phenology Network and North Central Climate Science Center (cooperative agreement number G16AC00224 from the United States Geo-logical Survey). Additional funding, through the National Science Foundation's LTER program, has supported research at Harvard Forest (DEB-1237491) and Bartlett Experimental Forest (DEB-1114804). We also thank the USDA Forest Service Air Resource Management program and the National Park Service Air Resources program for contributing their camera imagery to the PhenoCam archive.

Research at ARSMorris1 and ARSMorris2 is funded by the USDA-Agricultural Research Service (ARS) Project Number 5060-11610-003-00D of the Soil and Air National Program and Project number 5060-21220-006-00-D of the Crop Production National Program in coordination with the Long-term Agroecosystem Research (LTAR) network. We would like to thank Chris Wente and Steve Wagner for their role in the PhenoCam Network.

This research at the Jornada Experimental Range is funded by the USDA-Agriculture Research Service (ARS) via ARS Project Number 3050-11210-007-00D. Select camera locations are co-located with sites funded by National Science Foundation under Grant number DEB 1235828 as part of the Jornada Basin LTER program to New Mexico State University.

This research was supported in part by an appointment to the Agricultural Research Service (ARS) Research Participation Program administered by the Oak Ridge Institute for Science and Education (ORISE) through an interagency agreement between the U.S. Department of Energy (DOE) and the U.S. Department of Agriculture (USDA), Agricultural Research Service Agreement #60-3098-0-002.

COMPETING INTERESTS

Authors have declared that no competing interests exist.

REFERENCES

1. Seyednasrollah B, Richardson AD, Hufkens K, Milliman T, Aubrecht DM, Chen M, Gray JM, Johnston MR, Keenan TF, Klosterman ST, et al. PhenoCam dataset

v2.0: Vegetation Phenology from Digital Camera Imagery; 2000-2018.
2. Richardson AD, Jenkins JP, Braswell BH, Hollinger DY, Ollinger SV, Smith ML. Use of digital webcam images to track spring green-up in a deciduous broadleaf forest. Oecologia. 2007;152: 323–334. DOI:10.1007/s00442-006-0657-z
3. D'Odorico P, Gonsamo A, Gough CM, Bohrer G, Morison J, Wilkinson M, Hanson PJ, Gianelle D, Fuentes JD, Buchmann N. The match and mismatch between photosynthesis and land surface phenology of deciduous forests. Agric. For. Meteorol. 2015;214–215:25–38. DOI:10.1016/j.agrformet.2015.07.005
4. Sakamoto T, Gitelson AA, Nguy-Robertson AL, Arkebauer TJ, Wardlow BD, Suyker AE, Verma SB, Shibayama M. An alternative method using digital cameras for continuous monitoring of crop status. Agric. For. Meteorol. 2012;154–155:113. DOI:10.1016/j.agrformet.2011.10.014
5. Toda M, Richardson AD. Estimation of plant area index and phenological transition dates from digital repeat photography and radiometric approaches in a hardwood forest in the Northeastern United States. Agric. For. Meteorol. 2018;249:457–466. DOI:10.1016/j.agrformet.2017.09.004
6. Lukina EV, Stone ML, Raun WR. Estimating vegetation coverage in wheat using digital images. J. Plant Nutr; 1999. DOI:10.1080/01904169909365631
7. Browning DM, Snyder KA, Herrick JE. Plant phenology: Taking the pulse of rangelands. Rangelands; 2019. DOI:10.1016/j.rala.2019.02.001
8. Hufkens K, Keenan TF, Flanagan LB, Scott RL, Bernacchi CJ, Joo E, Brunsell NA, Verfaillie J, Richardson AD. Productivity of North American grasslands is increased under future climate scenarios despite rising aridity. Nat. Clim. Chang; 2016. DOI:10.1038/nclimate2942.
9. Grassland Soil and Water Research Laboratory: Temple TX ALMANAC Simulation Model Available:https://www.ars.usda.gov/plains-area/temple-tx/grassland-soil-and-water-research-laboratory/docs/193226/ (accessed on Oct 27, 2020).
10. Monsi M, Saeki T. Uber den Lichtfaktor in den Pflanzengesellschaf- u ur die Stoffproduktion. Japanese J. Bot.; 1953. German.
11. Snyder KA, Wehan BL, Filippa G, Huntington JL, Stringham TK, Snyder DK. Extracting plant phenology metrics in a great basin watershed: Methods and considerations for quantifying phenophases in a cold desert. Sensors (Switzerland). 2016;16. DOI:10.3390/s16111948.
12. Keenan TF, Darby B, Felts E, Sonnentag O, Friedl MA, Hufkens K, O'Keefe J, Klosterman S, Munger JW, Toomey M, et al. Tracking forest phenology and seasonal physiology using digital repeat photography: A critical assessment. Ecol. Appl. 2014;24:1478–1489. DOI:10.1890/13-0652.1
13. USDA The Long-Term Agroecosystem Research Network. Available:https://ltar.ars.usda.gov/about/ (accessed on Oct 20, 2020)
14. Schneider CA, Rasband WS, Eliceiri KW. NIH Image to ImageJ: 25 years of image analysis. Nat. Methods; 2012.
15. The University of New Hampshire The Phenocam Network. Available:https://phenocam.sr.unh.edu/webcam/about/ (accessed on Oct 26, 2020).
16. Soil Survey Staff Web Soil Survey. Available: http://websoilsurvey.nrcs.usda.gov/.
17. Nijland W, de Jong R, de Jong SM, Wulder MA, Bater CW, Coops NC. Monitoring plant condition and phenology using infrared sensitive consumer grade digital cameras. Agric. For. Meteorol. 2014;184:98–106. DOI:10.1016/j.agrformet.2013.09.007.
18. Reid AM, Chapman WK, Prescott CE, Nijland W. Using excess greenness and green chromatic coordinate colour indices from aerial images to assess lodgepole pine vigour, mortality and disease occurrence. For. Ecol. Manage. 2016;374:146–153. DOI:10.1016/j.foreco.2016.05.006.
19. Brown TB, Hultine KR, Steltzer H, Denny EG, Denslow MW, Granados J, Henderson S, Moore D, Nagai S, Sanclements M, et al. Using phenocams to monitor our changing earth: Toward a global phenocam network. Front. Ecol. Environ.; 2016.
20. Sonnentag O, Hufkens K, Teshera-Sterne C, Young AM, Friedl M, Braswell BH, Milliman T, O'Keefe J, Richardson AD.

Digital repeat photography for phenological research in forest ecosystems. Agric. For. Meteorol.; 2012. DOI:10.1016/j.agrformet.2011.09.009.
21. Dillen SY, de Beeck MO, Hufkens K, Buonanduci M, Phillips NG. Seasonal patterns of foliar reflectance in relation to photosynthetic capacity and color index in two co-occurring tree species, Quercus rubra and Betula papyrifera. Agric. For. Meteorol. 2012;160:60–68. DOI:10.1016/j.agrformet.2012.03.001
22. Browning DM, Karl JW, Morin D, Richardson AD, Tweedie CE. Phenocams bridge the gap between field and satellite observations in an arid grassland ecosystem. Remote Sens. 2017;9: DOI:10.3390/rs9101071.
23. Aasen H, Kirchgessner N, Walter A, Liebisch F. PhenoCams for field phenotyping: Using very high temporal resolution digital repeated photography to investigate interactions of growth, phenology, and harvest traits. Front. Plant Sci. 2020;11:1–16. DOI:10.3389/fpls.2020.00593.
24. Baldevbhai PJ. Color Image Segmentation for Medical Images using L*a*b* Color Space. IOSR J. Electron. Commun. Eng. 2012;1:24–45. DOI:10.9790/2834-0122445.
25. Ferreira T, Rasband W. ImageJ user guide user guide ImageJ. Image J user Guid; 2012. DOI:10.1038/nmeth.2019.
26. NOAA National Oceanic and Atmospheric Administration Climate Data Online Search. Available:http://ncdc.noaa.gov/cdo-web/search
27. Anderson J. Jornada Basin LTER: Wireless meteorological station at NPP M-NORT site: 1-hour summary data: 2013 - ongoing ver 15.
28. Anderson J. Jornada Basin LTER: Wireless meteorological station at NPP C-SAND site: 1-hour summary data: 2013 - ongoing ver 15.
29. Anderson J. Jornada Basin LTER: Wireless meteorological station at NPP G-IBPE site: 1-hour summary data: 2013 - ongoing ver 14.
30. USDA NRCS National Water and Climate Center, New Mexico SCAN Site Jornada Exp Rangeo Title. Available:https://wcc.sc.egov.usda.gov/nwcc/site?sitenum=2168.
31. USDA ARS Riesel Climatic data. Available:https://www.ars.usda.gov/plains-area/temple-tx/grassland-soil-and-water-research-laboratory/docs/riesel-climatic-data/
32. Kiniry JR, Burson BL, Evers GW, Williams JR, Sanchez, H, Wade, C, Featherston, J.W, Greenwade, J. Coastal bermudagrass, bahiagrass, and native range simulation at diverse sites in Texas. In Proceedings of the Agronomy Journal; 2007.
33. Kim S, Jeong J, Kiniry JR. Simulating the productivity of desert woody shrubs in Southwestern Texas. Arid Environ. Sustain; 2018. DOI:10.5772/intechopen.73703
34. Sunoj S, Igathinathane C, Hendrickson J. Monitoring plant phenology using phenocam: A review. In Proceedings of the 2016 American Society of Agricultural and Biological Engineers Annual International Meeting, ASABE 2016; 2016.
35. Iiames JS, Cooter E, Pilant AN, Shao Y. Comparison of EPIC-simulated and MODIS-derived leaf area index (LAI) across multiple spatial scales. Remote Sens. 2020;12:1–22. DOI:10.3390/RS12172764.
36. Schrader-Patton, C, Grulke, N.E, Ott, J. Monitoring land surface phenology in near real time by using phenomap. USDA For. Serv. - Gen. Tech. Rep. PNW-GTR. 2020;2020:1–104.

Peer-review history:
The peer review history for this paper can be accessed here:
http://www.sdiarticle4.com/review-history/69364